5.4 System Throughputs

Jared R. Males

1 Introduction

This section documents our analysis of the system throughputs of the as-designed system. The key quantity is the photon rate (photons/sec) delivered to each of the detector planes in the system. These are the high-order wavefront sensor (HOWFS), the low-order WFS (LOWFS), and the two SDI science cameras.

The requirements to be met by this analysis are that it is complete (considers all main sources of throughput loss) and that it is realistic. This ensures that we can adequately analyze and simulate system performance. There are no required values on the final system throughput.

2 Coatings

The following coatings were considered:

- Primary and Secondary: protected Aluminum

- Tertiary: a custom coating with enhanced reflectivity near 0.8 μm.

- OAPs and Flats: protected Silver, using a curve provided by Thor Labs.

- Alpao DMs: same protected Silver curve.

- BMC MEMS DM: unprotected gold

- Transmissive surfaces: a standard anti-reflective coating.

The coating reflectance and transmission profiles are shown in Figure 1.

3 Cameras

The quantum efficiency (QE) curves for the First Light Imaging OCAM-2K (HOWFS detector) and the Andor iXon 897 (LOWFS detector) and 888 (Science detectors) were digitized from the manufacturer specification sheets. These are shown in Figure 2.

4 Filters

The following filters were designed for the Hα configuration

- A dichroic beamsplitter which divides the light between the HOWFS and Science channels. Cuts-on at 0.68 μm, with T and R both 95%.

- A LOWFS filter which selects only in-band light of the vAPP leakage term, including the 5% leakage term.

- An Hα SDI filter set, as quoted by a vendor (see Opto-Mechanical design for details).

These curves are shown in Figure 3.
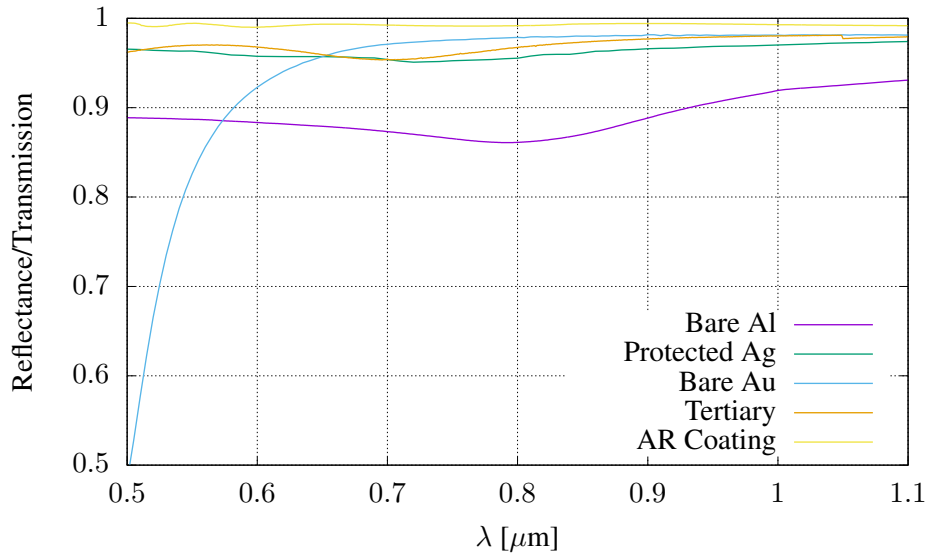
Figure 1: Reflectance and transmission profiles of coatings assumed.
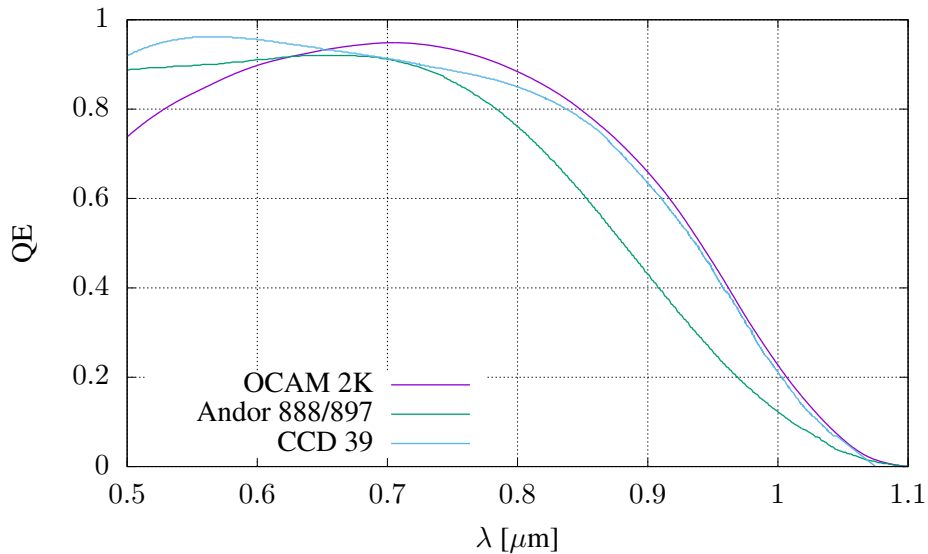
Figure 2: QE curves of the cameras to be used in MagAO-X.

5 Atmosphere

We include atmospheric transmission calculated using the BTRAM IDL code. We assumed 5.0 mm precipitable water vapor (PWV), and observing at zenith distance 30°, or airmass 1.15. The calculated telluric transmission is
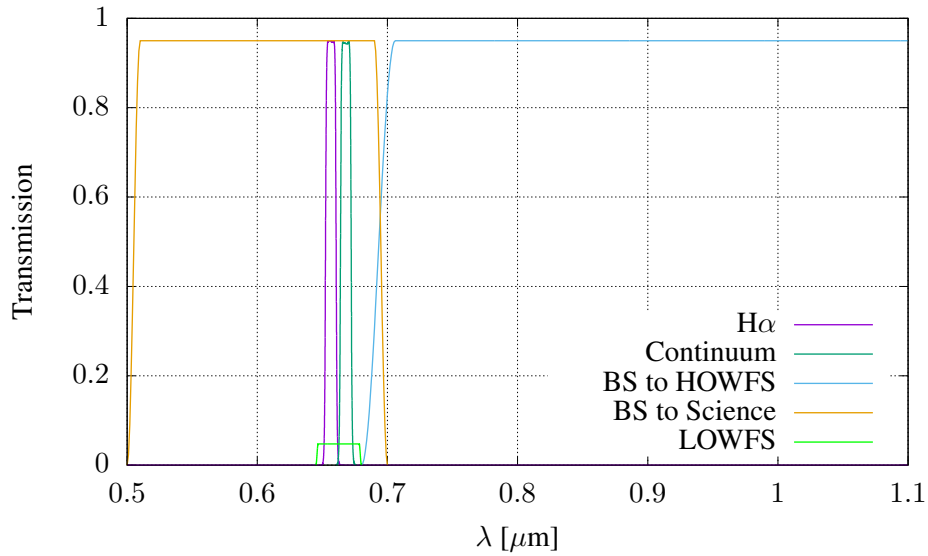
Figure 3: Filter curves designed for MagAO-X.

shown in Figure 4.
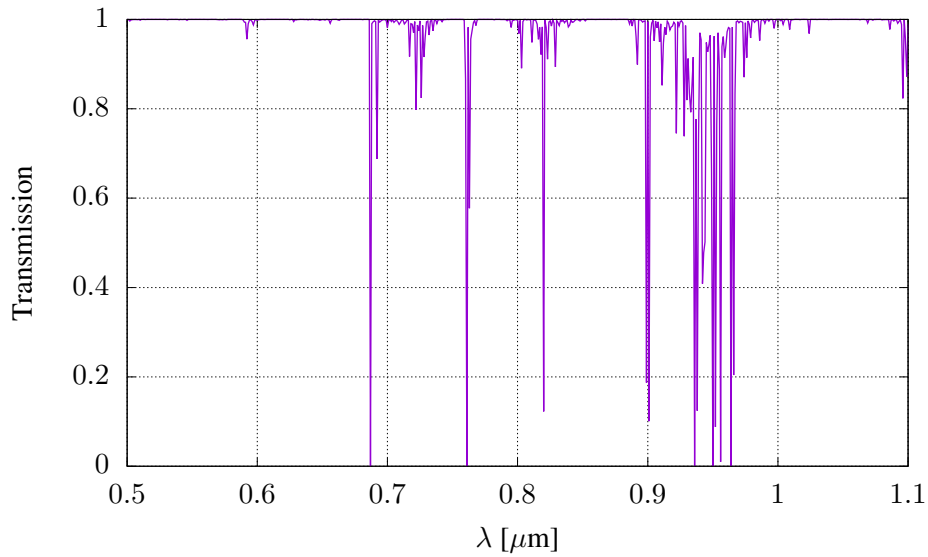
Figure 4: Atmospheric transmission for LCO calculated with BTRAM. Assumed 5.0 mm PWV and 30° zenith distance (airmass 1.15).

MagAO-X Preliminary Design
5.4 System Throughputs

Doc #:	MagAOX-001
Date:	2017–04–23
Status:	
	Rev. 0.2
Page:	4 of 6

6 Transmission Characteristics and Throughputs

Finally, the complete transmission curves for each of the planes in the Hα configuration was calculated by multiplying the above curves. This the reflectance or transmittance for each optic in the system, the atmosphere, the detector QE, and the appropriate filter curves. We also included a 10% loss due to diffraction derived from the Fresnel propagation analysis. These final transmission curves are shown in Figure 5.
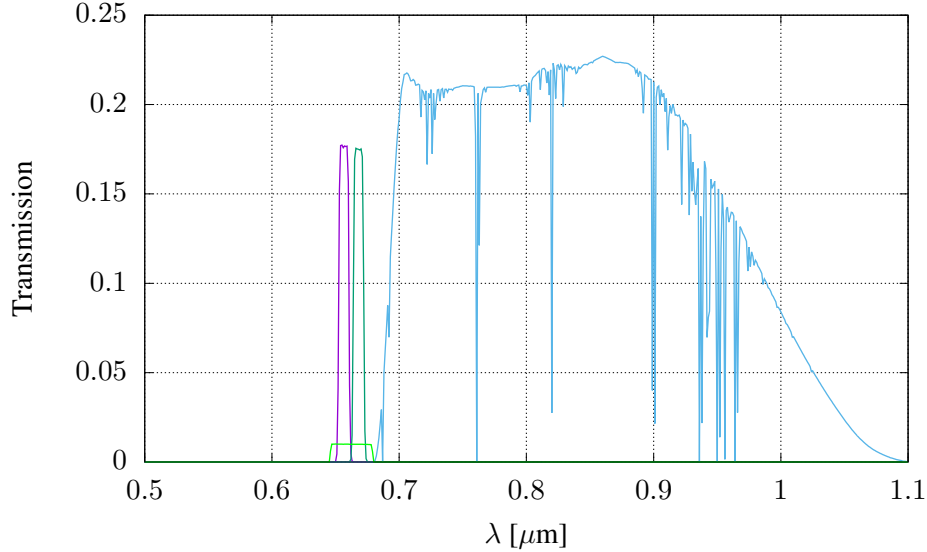
Figure 5: The final transmission curves for MagAO-X at each of the detector planes.

We then characterized each filter. We declare the throughput η of each filter to be the peak of the curve shown in Figure X. For each final filter curve, we converted to photon-weighted "relative spectral response" following Bessell (2000):

$$T(\lambda) = \frac{1}{hc}\lambda T_0(\lambda)$$

where T_0 is the raw energy-weighted profile. We also normalized these curves have a peak of 1. The central wavelength is

$$\lambda_0 = \frac{\int_0^\infty \lambda T(\lambda)d\lambda}{\int_0^\infty T(\lambda)d\lambda}$$

Using the Vega spectrum of Bohlin (2007), we determine the photon flux-density of a 0 magnitude star at 100% in each filter from

$$F_\lambda(\lambda_0) = \frac{\int_0^\infty F_\lambda(\lambda)T(\lambda)d\lambda}{\int_0^\infty T(\lambda)d\lambda}$$

and the effective width $\Delta\lambda$ from

$$\Delta\lambda = \int_0^\infty T(\lambda)d\lambda$$

4

such that the total photon flux in the filter is

$$F_\lambda(\lambda_0)\Delta\lambda = \int_0^\infty F_\lambda(\lambda)T(\lambda)d\lambda.$$

Finally, we have the total 0-magnitude photon rate at a given plane in the MagAO-X system

$$F_\gamma(0) = F_\lambda(\lambda_0)\Delta\lambda A\eta$$

where A is the collecting area of the telescope. We included the central obscuration, and for the planes downstream of the coronagraph we took into account the undersized mask.

The resultant filter characteristics are shown in Table 1.

Table 1: Final filter characteristics for the Hα configuration.

| Plane | Throughput | λ_0 | $\Delta\lambda$ | $F_\gamma(0)$ | Notes |
		μm	μm	Photons/sec	
Science Hα	0.177	0.657	0.0082	2.3×10^9	
Science Cont.	0.176	0.668	0.0083	2.6×10^9	
LOWFS	0.010	0.662	0.033	5.9×10^8	5% vAPP leakage
HOWFS	0.227	0.851	0.257	7.6×10^{10}	

7   Throughputs for the f/16 ASM feed

The operation of MagAO-X with the f/16 ASM will require splitting photons between the MagAO WFS and the MagAO-X WFS. We plan to employ a set of selectable dichroic beamsplitters. These will reflect some fraction of photons into the existing MagAO system (as Clio2's entrance window does now) and transmit the remaining photons to MagAO-X. Here we analyze the Hα science case. Here, 100% of the light short of 680 nm will transmitted into MagAO-X. Longer than 680, 25% is reflected to MagAO, and 75% is transmitted to MagAO-X. These red photons will be used for wavefront sensing.

We also consider the transmissions and reflections in the optical train for each system, as above. For MagAO, we include the various surfaces after the dichroic, assume no beamsplitter is used internal to the MagAO WFS, and use the CCD 39 detector QE.

The resultant transmission curves for each system are shown in Figure 6. These curves were then integrated over the spectrum of Vega to determine the 0-magnitude photon rate for each part of the MagAO+MagAO-X system. These are given in Table 2.

References

Bessell, M. S. 2000, PASP, 112, 961

Bohlin, R. C. 2007, in Astronomical Society of the Pacific Conference Series, Vol. 364, The Future of Photometric, Spectrophotometric and Polarimetric Standardization, ed. C. Sterken, 315
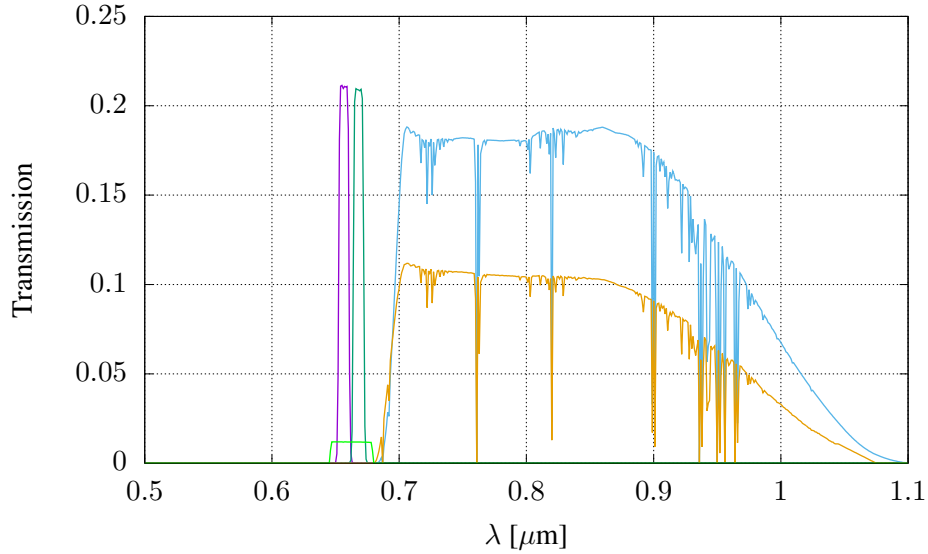
Figure 6: The final transmission curves for MagAO-X+f/16 at each of the detector planes. The gold curve corresponds to the MagAO WFS.

Table 2: Zero-magnitude fluxes for MagAO and MagAO-X for the $H\alpha$ science case

Plane	Throughput	λ_0	$\Delta\lambda$	$F_\gamma(0)$	Notes
		μm	μm	Photons/sec	
Science $H\alpha$	0.211	0.657	0.0082	2.8×10^9	
Science Cont.	0.21	0.668	0.0083	3.2×10^9	
LOWFS	0.012	0.663	0.033	7.0×10^8	
HOWFS	0.188	0.85	0.258	6.3×10^{10}	
MagAO-WFS	0.112	0.842	0.261	3.9×10^{10}	